

Algorithmic Primitives for Quantum-Assisted Quantum Control

Guru-Vamsi Policharla¹ and Sai Vinjanampathy^{1,2,*}

¹*Department of Physics, Indian Institute of Technology-Bombay, Powai, Mumbai 400076, India.*

²*Centre for Quantum Technologies, National University of Singapore, 3 Science Drive 2, Singapore 117543, Singapore*

(Dated: November 30, 2020)

We discuss two primitive algorithms to evaluate overlaps and transition matrix time series, which are used to construct a variety of quantum-assisted quantum control algorithms implementable on NISQ devices. Unlike previous approaches, our method bypasses tomographically complete measurements and instead relies solely on single qubit measurements. We analyse circuit complexity of composed algorithms and sources of noise arising from Trotterization and measurement errors.

Introduction.— Quantum control is central to the design of quantum technologies [1]. The control problem usually involves optimising a cost function that incorporates conditions such as distance to a target state, bandwidth and fluence restrictions. The problem is then solved by employing gradient search methods [2–6], non-gradient search methods [7–16] or hybrid algorithms [17]. Such solutions typically involve several iterative updates to the controls before convergence to a local optima. Since these methods simulate quantum evolution on a classical computer repeatedly, often the time complexity for many-body quantum control protocols is dominated by the corresponding complexity of the evolution.

Several techniques to partially overcome the computational intractability have been developed. For instance, mean-field and cumulant expansion theories [18, 19] have been used in the place of the full evolution. However, the approximations are either limited or uncontrolled. Another recent approach [20] has been to use matrix product state approaches embedded inside control algorithms. Though this simulates a larger set of quantum states on a classical computer, such techniques cannot efficiently compute generic quantum evolution.

Given the advances in noisy intermediate-scale quantum computing (NISQ) [21, 22] platforms, a potential solution is to simulate quantum evolution on NISQ devices and extract control pulses via measurements. This problem has been considered before, though the solutions have been limited. For instance, hybrid GRAPE algorithm was proposed [23, 24] and implemented [25] for optimal control. The evolution of states is done on a quantum simulator and the cost function and its gradients are estimated by projecting the final density matrix into specific quantum states. This technique is limited by the fact that the number of projectors needed to span an arbitrary density matrix basis is exponential in the number of qubits. To mitigate this, previous authors typically restrict the target states to sparse matrices in the measurement basis, which in turn restricts the possible control solutions one can obtain.

In this manuscript, we propose the first control solution for state optimisation that is applicable to dense target states by adapting existing techniques from quan-

tum computation and expanding them to compose two *algorithmic primitives*. They can be implemented on a universal quantum computer, provided the many-body target states are available as an offline resource. This demand for an offline resource is justified since our method is akin to compilation of quantum circuits, where an optimal gate decomposition of a given unitary in terms of a universal gate set is sought. Our method is related to these quantum gate compilation techniques [26–28] in seeking optima but are significantly different since the underlying unitary is also being optimized for a fixed target state.

The main insight of our work is that most optimal control techniques such as Krotov [2], GRAPE [3], CRAB [12, 13] and machine learning methods [7] only require certain scalars in their update step (as opposed to a description of the entire state). We propose schemes to extract these scalars, which are either in the form of the overlap of two states $\langle\psi(t)|\chi(t)\rangle$ or the transition element between two states in a fixed Hermitian operator of the form $\langle\chi(t)|\mu|\psi(t)\rangle$ using a digital quantum simulator (DQS) and qubit measurements. A schematic illustration of our quantum-assisted quantum control algorithm can be found in Fig.(1).

Overlap Estimation Algorithm (OEA).— Consider two time-dependent many-body quantum states $|\psi(t)\rangle = U(t)|\psi_0\rangle$ and $|\chi(t)\rangle = V(t)|\chi_0\rangle$ generated by the evolution operators which are Trotterized implementations of a time-continuous control sequence discussed below. Given these two (generic) states, we wish to estimate the overlap $\langle\chi(t)|\psi(t)\rangle$. It is well known that if we were given the bipartite state $|x\rangle := (|0\rangle|\psi(t)\rangle + |1\rangle|\chi(t)\rangle)/\sqrt{2}$, the real part of the overlap $\langle\chi(t)|\psi(t)\rangle$ can be evaluated by measuring the detection probability of $|1\rangle$ on the first (ancillary) qubit of the state $H \otimes \mathbb{I}|x\rangle$, where H denotes the Hadamard gate. Likewise, the imaginary part of the overlap can be obtained by starting with $|x'\rangle := (|0\rangle|\psi(t)\rangle - i|1\rangle|\chi(t)\rangle)/\sqrt{2}$. We next outline a method to generate such superpositions.

To create superpositions between unknown states, we first extend the results of Oszmaniec et al. [29], who

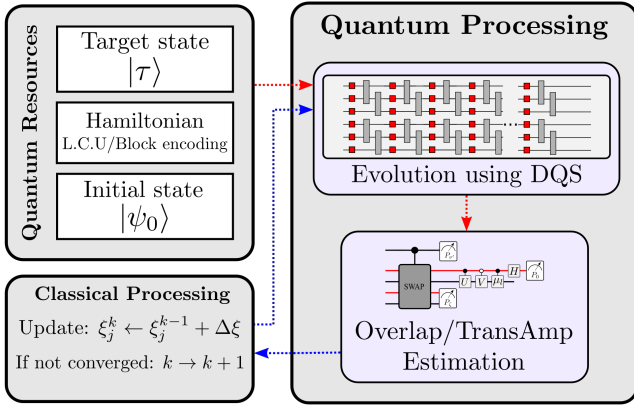


FIG. 1: A high level schematic of our quantum-assisted quantum control algorithms where scalars are extracted using OEA and TAEA given target and Hamiltonian resources.

proposed a probabilistic CP map Λ_{sup} to superpose any two given states $|\psi\rangle$ and $|\chi\rangle$ which have a non-zero overlap with a given reference state $|\zeta\rangle$. Concretely, their algorithm takes as input $|\nu\rangle = \alpha|0\rangle + \beta|1\rangle$, $|\psi\rangle$ and $|\chi\rangle$ to generate states of the form

$$\alpha \frac{\langle\psi|\zeta\rangle}{|\langle\psi|\zeta\rangle|} |\psi\rangle + \beta \frac{\langle\chi|\zeta\rangle}{|\langle\chi|\zeta\rangle|} |\chi\rangle, \quad (1)$$

using well known post-selection methods [30], as incorporated in Fig.(2). If the overlaps are known, then the additional phase factor can be removed by modifying α and β appropriately. Our extension generates arbitrary superpositions of states $|\psi(t)\rangle = U(t)|\psi\rangle$ and $|\chi(t)\rangle = V(t)|\chi\rangle$ as follows: If a reference state $|\zeta\rangle$ and overlaps $\langle\chi|\zeta\rangle \neq 0$ and $\langle\psi|\zeta\rangle \neq 0$ are known, Λ_{sup} can be used to create a probabilistic superposition of the form $\alpha|0\rangle|\psi\rangle + \beta|1\rangle|\chi\rangle$ by choosing a reference state $|+\rangle|\zeta\rangle$ and inputs $|0\rangle|\psi\rangle$ and $|1\rangle|\chi\rangle$. Then by applying conditional unitaries $|0\rangle\langle 0| \otimes U(t) + |1\rangle\langle 1| \otimes V(t)$, we obtain states of the form

$$|\Psi\rangle = \alpha|0\rangle U(t)|\psi\rangle + \beta|1\rangle V(t)|\chi\rangle. \quad (2)$$

We note that superpositions of $U(t)|\psi\rangle$ and $V(t)|\phi\rangle$ can be created by applying a Hadamard on the first qubit and measuring it in the standard basis. If $\alpha = |\langle\psi|\zeta\rangle|/(\sqrt{2}|\langle\psi|\zeta\rangle|)$ and $\beta = |\langle\chi|\zeta\rangle|/(\sqrt{2}|\langle\chi|\zeta\rangle|)$, the output is the desired state $|x\rangle = (|0\rangle|\psi(t)\rangle + |1\rangle|\chi(t)\rangle)/\sqrt{2}$. Choices of the generic quantum states specify various control algorithms discussed below. For instance, the choice of $|\psi\rangle \equiv |\psi_0\rangle$ to be the initial quantum state and $|\chi\rangle \equiv |\tau\rangle$ to be the target state respectively will specify the Krotov algorithm discussed below. This method can also be used to construct several other examples of gradient-based and gradient-free control algorithms. In all such control algorithms, we choose the reference state $|\zeta\rangle$ to be a sparse quantum state with non-zero overlap with the initial and target state. For instance, $|\zeta\rangle$ can

be chosen to be a sparse initial state if it has non-zero overlap with the target state. We note that this choice of the reference state is not unique and can be chosen according to experimental convenience. This reduces the problem of superposition of two unitarily rotated states to the problem of applying arbitrary control unitary on an unknown state.

Following Zhou *et. al.*, [31] we can add control to arbitrary unitaries U and V by padding them with controlled- X_a or *internal-SWAP* gates. The X_a gate has been experimentally demonstrated for photonic systems [23] and requires that each qubit state be the lower energy manifold of an otherwise controllable multi-level system. This is naturally also the case for transmon qubits [32–35] and several other physical implementations of universal quantum computers. For a four level system, the X_a gate is defined by the transformation rules $|0\rangle \leftrightarrow |2\rangle$, $|3\rangle \leftrightarrow |1\rangle$. For larger Hilbert spaces it can be defined via a SWAP gate that acts internally on subspaces of the same Hilbert space, distinguishing it from the usual SWAP gate that acts on tensor product spaces. This doubles the internal Hilbert space dimensionality of the physical qubit to add control scaling linearly with the number of subsystems.

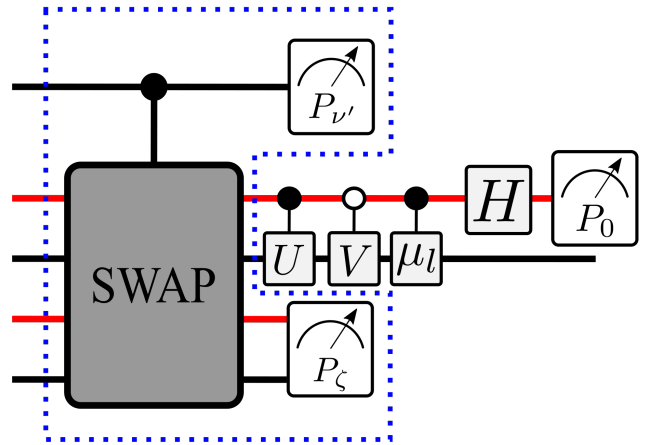


FIG. 2: A circuit for estimating transition amplitudes of the form $\langle\tau|V^\dagger\mu U|\psi_0\rangle$ using the LCU technique. Using D conditional unitaries μ_l , the transition amplitude can be estimated. The circuit inside the dotted box is an implementation of Λ_{sup} for superposing states where $|\nu\rangle = |\langle\psi|\zeta\rangle||0\rangle + |\langle\chi|\zeta\rangle||1\rangle$.

Transition Amplitude Estimation Algorithm (TAEA).— The second timeseries we require for the control algorithms is the estimation of transition matrix elements of the form $\langle\chi(t)|\mu|\psi(t)\rangle$. If the Hamiltonian μ can be expressed as a linear combination of known unitaries [36] $\mu = \sum_{l=1}^D c_l \mu_l$, then by applying a conditional unitary μ_l on $|\Psi\rangle$ we can estimate the

overlap $\langle \chi(t) | \mu | \psi(t) \rangle$ and hence $\langle \chi(t) | \mu | \psi(t) \rangle$. This is presented in Fig. (2) in terms of a circuit description.

Alternatively, if there exists a block encoding [37, 38] $B \in \mathbb{C}^k \otimes \mathcal{H}$ of $\mu \in \mathcal{H}$, then by applying a conditional version of this unitary on $(|0\rangle |0_k\rangle |\psi(t)\rangle + |1\rangle |0_k\rangle |\chi(t)\rangle) / \sqrt{2}$, we can estimate $\langle \psi(t) | \langle 0_k | B | 0_k \rangle | \chi(t) \rangle$ and hence $\langle \psi(t) | \mu | \chi(t) \rangle$ (See appendix A for a formal algorithmic description of these primitives).

Quantum-Assisted Gradient Algorithms.— Let us apply these algorithmic primitives to construct quantum-assisted quantum control algorithms. Consider quantum control algorithms that operate with fixed terminal time (T) such as Krotov’s algorithm [2]. Without loss of generality we work with Hamiltonians of the form $H(t) = H_0 + \xi(t)\mu$ where $H_0(\mu)$ is the bare(control) Hamiltonian. The cost function in the Krotov algorithm is given by

$$J = \langle \psi(T) | Q | \psi(T) \rangle - \alpha \int_0^T dt \xi^2(t), \quad (3)$$

where $Q = |\tau\rangle \langle \tau|$ is the projector onto the target state $|\tau\rangle$. Here the integral represents the fluence of the control field $\xi(t)$ and α is a Lagrange multiplier that modulates the relative importance of the second term. The first order variation of the cost function produces three equations of motion

$$|\dot{\psi}^{(k)}(t)\rangle = -iH^{(k)} |\psi^{(k)}(t)\rangle, \quad (4)$$

$$|\dot{\chi}^{(k)}(t)\rangle = -iH^{(k)} |\chi^{(k)}(t)\rangle, \quad (5)$$

$$\Delta \xi^{(k)}(t) = -\frac{1}{\alpha} \text{Im} \langle \chi^{(k-1)}(t) | \mu | \psi^{(k)}(t) \rangle, \quad (6)$$

which are solved iteratively subject to the boundary conditions $|\psi^{(k)}(0)\rangle = |\psi_0\rangle$ and $|\chi^{(k)}(T)\rangle = Q |\psi^{(k)}(T)\rangle$ until convergence is reached. Here $H^{(k)}(t) = H_0 + \xi^{(k)}(t)\mu$ is the time-dependent Hamiltonian with the control field $\xi^{(k)}(t)$, state $|\psi^{(k)}(t)\rangle$ and co-state $|\chi^{(k)}(t)\rangle$ corresponding to the k^{th} iteration of the algorithm. Each iteration of the solution proceeds by evolving the state and co-state equations alongside computing the overlap integral. Note that the state equation Eq. (4) is specified by an initial condition whereas the co-state equation Eq. (5) is specified by a terminal condition. This implies that while the state equation is evolved forward in time, the co-state equation is evolved backward in time.

By using OEA and TAEA we can implement a quantum-assisted Krotov algorithm that circumvents the exponential complexity of simulating state evolution. Throughout the algorithm we only use superpositions of the form $|y\rangle = \alpha |0\rangle |\psi(0)\rangle + \beta |1\rangle |\tau\rangle$ which can be prepared as described earlier if the overlaps with respect to some reference state are known. Evolution of states is done according to Eq. (4) and Eq.(5) via digital quantum simulation which can be done efficiently even for many body systems. Note that since $|\chi(t)\rangle = V(t) |\chi(T)\rangle =$

$\langle \tau | \psi(T) \rangle V(t) |\tau\rangle$, we need to estimate the scalar overlap $\langle \tau | \psi(T) \rangle$ which can be done using OEA given $|y\rangle$. To compute the control field updates $\Delta \xi^{(k)}(t)$ we employ TAEA. Other popular algorithms such as GRAPE can also be implemented in a quantum assisted fashion (see appendix B).

Quantum-Assisted Gradient-free Algorithms.— Besides gradient algorithms, OEA and TAEA can be used to also implement non-gradient quantum control algorithms. As an example, we consider the Chopped Random Basis (CRAB) Optimisation [12] which works by performing a search on a truncated basis. The candidate control field is written as $\xi(t) = \sum_{i=1}^N c_i \xi_i(t)$ where ξ_i ’s are typically trigonometric functions. The coefficients c_i are optimised using standard non-gradient techniques such as Nelder-Mead algorithm [39] to obtain the optimal pulse sequences. Since the Nelder-Mead technique uses the function to be optimised in a black-box fashion the only quantity that needs to be extracted is the fidelity which is done using a SWAP test [40]. Likewise, the dCRAB technique [13] and machine learning based control algorithms such as SuSSADE [7] can be assisted by a quantum simulator since the only relevant quantity needed for optimization is fidelity.

Resource Counting— Our algorithmic primitives use m repeated single-qubit measurements to estimate scalar values, which we group into a single *experiment* and begin the complexity analysis with the number of experiments needed for several example algorithms. We then separately estimate the relationship between Trotter error, number of measurement repetitions and the error threshold per experiment. The superposition part of either primitive requires measurements in a basis containing the reference state $|\zeta\rangle$ which can be done easily if a unitary transformation can be implemented such that it takes some standard basis state to $|\zeta\rangle$. The OEA requires two experiments, one each for estimating real and imaginary parts. The number of experiments for TAEA depends on the approach used. While block encoding only needs two experiments, LCU requires $2D$ experiments one each for the real and imaginary parts of D different terms in the LCU decomposition of the operator μ . The number of times each quantum-assisted control algorithm invokes the algorithmic primitives can be inferred simply. For each update, one TAEA experiment and two OEA experiments are needed. Quantum-assisted GRAPE requires two fidelity experiments in each update step.

We now relate the error thresholds to the number of measurements m and pulse updates n by focusing on the quantum-assisted Krotov algorithm, the extension of this analysis to other algorithms being straightforward. We consider two sources of error, the first is due to Trotterization which results in an approximate version of the unitary corresponding to time evolution being implemented and the second is due to the finite precision arising from

a finite number of measurements. Since the Krotov algorithm has the property of monotonic convergence, the quantum-assisted Krotov algorithm enjoys this property as well up until the point where the incremental change in the cost function $\Delta J^{(k)} = J^{(k)} - J^{(k-1)}$ in an ideal implementation is comparable to the fluctuation in $\Delta J^{(k)}$ due to the two sources of errors mentioned above. Poulin et al. [41] upper bound the error of a Hamiltonian written as the sum of L terms $H(t) = \sum_{i=1}^L H_i(t)$ with bounded norm. Assuming each term acts on at most κ qubits, the total error in approximating the exact time evolution is upper bounded by

$$\|U - U^{\text{TS}}\| = \varepsilon_{TS} \leq \frac{c_{max}^2 T^2}{2n^2} \quad (7)$$

where $n = T/\Delta t$, T is the total time of evolution, Δt is the time interval over which Hamiltonian fluctuation is negligible, $\|\cdot\|$ denotes Hamiltonian norm, $c_{max} = \max_t \max_i \|H_i(t)\|$, $U = \mathcal{T} \exp\{-i/\hbar \int_0^T H(t) dt\}$ is the time ordered integral and U^{TS} is the Trotter-Suzuki implementation of U . The number of gates required to implement the Trotterized gates is given by $d_{sk} G(\varepsilon_{TS}, L, T) \log(G(\varepsilon_{TS}, L, T)/\varepsilon_{TS})^{c_{sk}}$ where d_{sk}, c_{sk} are Solovay-Kitaev constants and $G(\varepsilon_{TS}, L, T) = c_{max}^2 T^2 L^3 / \varepsilon_{TS}$. Thus choosing ε_{TS} fixes the total number of gates in the Trotter decomposition. We note that though we present upper limits to the number of gates, many-body localization was recently shown to stabilize local observables [42] for time-independent DQS with relatively small number of gate operations while retaining desired levels of accuracy, a result that directly applies to our protocols.

A second source of error we consider is due to the finite precision arising from a finite number of measurements. The number of runs of TAEA and OEA relates to the fluctuations in the pulse update $\Delta \xi_j^{(k)}$ and can be used to upperbound it using ε_M (see appendix C). Using this we are able to upperbound the fluctuations in $\Delta J^{(k)}$ due to the two sources of error. As long as the stochastically averaged change is larger than than the maximum fluctuation we are guaranteed monotonicity of the quantum-assisted Krotov algorithm. This condition can be written as

$$\langle\langle \Delta J^{(k)} \rangle\rangle \gg 4T\varepsilon \|\mu\| + 4\frac{T}{\alpha} [\xi_{max}\varepsilon] + 4\varepsilon_{TS} \quad (8)$$

where T is total time and ξ_{max} is the maximum value of the control field, $\varepsilon = \varepsilon_M + 3\varepsilon_{TS} \|\mu\|/\alpha$. Hence by setting a threshold on the stochastically averaged cost function $\langle\langle \Delta J^{(k)} \rangle\rangle$ below which we stop optimization, we can compute the required number of gates and measurements in terms of ε_{TS} and ε_M respectively. We note that for bounded Hamiltonians Eq. (8) suggests a reasonable scaling of number of gates and measurements needed to perform quantum-assisted quantum control.

Conclusions.— We present the algorithmic primitives OEA and TAEA to implement arbitrary quantum-assisted quantum control algorithms. Our method substantially improves existing hybrid quantum control algorithms by incorporating dense target states and complex control algorithms. Furthermore, the underlying algorithmic primitives only rely on qubit measurements and require the implementation of specific controlled unitaries, that can be accomplished by well known methods. We emphasize that the circuit complexity of specific algorithms considered scales favourably with error thresholds. We applied our method to quantum-assisted versions of gradient and non-gradient algorithms. Several recent experiments have demonstrated control of relatively large number of qubits on differing platforms, from gradient algorithm on twelve NMR qubits [25] to a controlled state preparation of twenty transmon qubits [43] suggesting that our protocols are practical to implement with existing technology. Furthermore, when two separate platforms can both simulate the same Hamiltonians H_0 and μ , our method can be combined with analog/digital quantum simulation experiments to design optimal control pulses in new systems. For example, proposals to generate all-optical higher-dimensional tensor network states [44, 45] can be used to generate complex target states for our scheme.

Our techniques add to the literature on variational quantum algorithms [46–48] and generalize the optimization program to complex overlaps which bring control theory objectives and variational quantum algorithms closer [49]. Furthermore, our algorithmic primitives can also be used to optimize non-gradient objectives and can be used for the important tasks such as the design of modular quantum computers [50–52] and controlling reactions in quantum chemistry [53].

Acknowledgements.— SV acknowledges support from the DST-SERB Early Career Research Award (ECR/2018/000957) and DST-QUEST grant number DST/ICPS/QuST/Theme-4/2019. SV thanks Kishor Bharti, Adolfo del Campo, Ish Dhand, Carlos Perez-Delgado and Dario Poletti for insightful discussions.

* sai@phy.iitb.ac.in

- [1] S. J. Glaser, U. Boscain, T. Calarco, C. P. Koch, W. Köckenberger, R. Kosloff, I. Kuprov, B. Luy, S. Schirmer, T. Schulte-Herbrüggen, *et al.*, The European Physical Journal D **69**, 1 (2015).
- [2] D. J. Tannor, V. Kazakov, and V. Orlov, in *Time-dependent quantum molecular dynamics* (Springer, 1992) pp. 347–360.
- [3] N. Khaneja, T. Reiss, C. Kehlet, T. Schulte-Herbrüggen, and S. J. Glaser, Journal of magnetic resonance **172**, 296 (2005).
- [4] P. Gross, D. Neuhauser, and H. Rabitz, The Journal of chemical physics **96**, 2834 (1992).

- [5] T. Szakács, B. Amstrup, P. Gross, R. Kosloff, H. Rabitz, and A. Lőrincz, *Physical Review A* **50**, 2540 (1994).
- [6] W. Zhu and H. Rabitz, *The Journal of Chemical Physics* **109**, 385 (1998).
- [7] E. Zahedinejad, J. Ghosh, and B. C. Sanders, *Physical Review Applied* **6**, 054005 (2016).
- [8] R. J. Spiteri, M. Schmidt, J. Ghosh, E. Zahedinejad, and B. C. Sanders, *New Journal of Physics* **20**, 113009 (2018).
- [9] F. Schäfer, M. Kloc, C. Bruder, and N. Lörch, *Machine Learning: Science and Technology* (2020).
- [10] M. Y. Niu, S. Boixo, V. N. Smelyanskiy, and H. Neven, *npj Quantum Information* **5**, 1 (2019).
- [11] M. Bukov, A. G. Day, D. Sels, P. Weinberg, A. Polkovnikov, and P. Mehta, *Physical Review X* **8**, 031086 (2018).
- [12] T. Caneva, T. Calarco, and S. Montangero, *Physical Review A* **84**, 022326 (2011).
- [13] N. Rach, M. M. Müller, T. Calarco, and S. Montangero, *Physical Review A* **92**, 062343 (2015).
- [14] P. Palittapongarnpim, P. Wittek, E. Zahedinejad, S. Vedaie, and B. C. Sanders, *Neurocomputing* **268**, 116 (2017).
- [15] A. Pechen and H. Rabitz, *Physical Review A* **73**, 062102 (2006).
- [16] S. Grivopoulos and B. Bamieh, in *42nd IEEE International Conference on Decision and Control (IEEE Cat. No. 03CH37475)*, Vol. 1 (IEEE, 2003) pp. 434–438.
- [17] M. H. Goerz, K. B. Whaley, and C. P. Koch, *EPJ Quantum Technology* **2**, 1 (2015).
- [18] Y.-C. Yang, S. N. Coppersmith, and M. Friesen, *Phys. Rev. A* **100**, 022337 (2019).
- [19] G. Jäger, D. M. Reich, M. H. Goerz, C. P. Koch, and U. Hohenester, *Physical Review A* **90**, 033628 (2014).
- [20] P. Doria, T. Calarco, and S. Montangero, *Physical review letters* **106**, 190501 (2011).
- [21] S. Boixo, S. V. Isakov, V. N. Smelyanskiy, R. Babbush, N. Ding, Z. Jiang, M. J. Bremner, J. M. Martinis, and H. Neven, *Nature Physics* **14**, 595 (2018).
- [22] E. Pednault, J. A. Gunnels, G. Nannicini, L. Horesh, T. Magerlein, E. Solomonik, and R. Wisnieff, *arXiv preprint arXiv:1710.05867* **15** (2017).
- [23] J. Li, X. Yang, X. Peng, and C.-P. Sun, *Physical review letters* **118**, 150503 (2017).
- [24] B. Dive, A. Pitchford, F. Mintert, and D. Burgarth, *Quantum* **2**, 80 (2018).
- [25] D. Lu, K. Li, J. Li, H. Katiyar, A. J. Park, G. Feng, T. Xin, H. Li, G. Long, A. Brodutch, *et al.*, *npj Quantum Information* **3**, 1 (2017).
- [26] N. Yu, R. Duan, and M. Ying, *Physical Review A* **88**, 010304 (2013).
- [27] J. J. Vartiainen, M. Möttönen, and M. M. Salomaa, *Physical review letters* **92**, 177902 (2004).
- [28] V. V. Shende, S. S. Bullock, and I. L. Markov, *IEEE Transactions on Computer-Aided Design of Integrated Circuits and Systems* **25**, 1000 (2006).
- [29] M. Oszmaniec, A. Grudka, M. Horodecki, and A. Wójcik, *Physical review letters* **116**, 110403 (2016).
- [30] K. Li, G. Long, H. Katiyar, T. Xin, G. Feng, D. Lu, and R. Laflamme, *Phys. Rev. A* **95**, 022334 (2017).
- [31] X.-Q. Zhou, T. C. Ralph, P. Kalasuwan, M. Zhang, A. Peruzzo, B. P. Lanyon, and J. L. O’Brien, *Nature communications* **2**, 1 (2011).
- [32] J. Koch, M. Y. Terri, J. Gambetta, A. A. Houck, D. Schuster, J. Majer, A. Blais, M. H. Devoret, S. M. Girvin, and R. J. Schoelkopf, *Physical Review A* **76**, 042319 (2007).
- [33] J. M. Gambetta, A. A. Houck, and A. Blais, *Phys. Rev. Lett.* **106**, 030502 (2011).
- [34] A. Mezzacapo, L. Lamata, S. Filipp, and E. Solano, *Phys. Rev. Lett.* **113**, 050501 (2014).
- [35] T. Roy, S. Kundu, M. Chand, S. Hazra, N. Nehra, R. Cosmic, A. Ranadive, M. P. Patankar, K. Damle, and R. Vijay, *Physical Review Applied* **7**, 054025 (2017).
- [36] A. M. Childs and N. Wiebe, *arXiv preprint arXiv:1202.5822* (2012).
- [37] G. H. Low and I. L. Chuang, *Quantum* **3**, 163 (2019).
- [38] A. Gilyén, Y. Su, G. H. Low, and N. Wiebe, in *Proceedings of the 51st Annual ACM SIGACT Symposium on Theory of Computing* (2019) pp. 193–204.
- [39] J. A. Nelder and R. Mead, *The computer journal* **7**, 308 (1965).
- [40] H. Buhrman, R. Cleve, J. Watrous, and R. De Wolf, *Physical Review Letters* **87**, 167902 (2001).
- [41] D. Poulin, A. Qarry, R. Somma, and F. Verstraete, *Physical review letters* **106**, 170501 (2011).
- [42] M. Heyl, P. Hauke, and P. Zoller, *Science advances* **5**, eaau8342 (2019).
- [43] C. Song, K. Xu, H. Li, Y.-R. Zhang, X. Zhang, W. Liu, Q. Guo, Z. Wang, W. Ren, J. Hao, H. Feng, H. Fan, D. Zheng, D.-W. Wang, H. Wang, and S.-Y. Zhu, *Science* **365**, 574 (2019).
- [44] M. Lubasch, A. A. Valido, J. J. Renema, W. S. Kolthammer, D. Jaksch, M. S. Kim, I. Walmsley, and R. García-Patrón, *Phys. Rev. A* **97**, 062304 (2018).
- [45] I. Dhand, M. Engelkemeier, L. Sansoni, S. Barkhofen, C. Silberhorn, and M. B. Plenio, *Phys. Rev. Lett.* **120**, 130501 (2018).
- [46] S. Khatri, R. LaRose, A. Poremba, L. Cincio, A. T. Sornborger, and P. J. Coles, *Quantum* **3**, 140 (2019).
- [47] Z.-C. Yang, A. Rahmani, A. Shabani, H. Neven, and C. Chamon, *Phys. Rev. X* **7**, 021027 (2017).
- [48] C. Lin, Y. Wang, G. Kolesov, and U. c. v. Kalabić, *Phys. Rev. A* **100**, 022327 (2019).
- [49] A. B. Magann, C. Arenz, M. D. Grace, T.-S. Ho, R. L. Kosut, J. R. McClean, H. A. Rabitz, and M. Sarovar, *arXiv preprint arXiv:2009.06702* (2020).
- [50] S. J. Devitt, A. G. Fowler, A. M. Stephens, A. D. Green-tree, L. C. Hollenberg, W. J. Munro, and K. Nemoto, *New Journal of Physics* **11**, 083032 (2009).
- [51] C. Arenz and H. Rabitz, *Physical review letters* **120**, 220503 (2018).
- [52] J. Lee, C. Arenz, D. Burgarth, and H. Rabitz, *Journal of Physics A: Mathematical and Theoretical* **53**, 125304 (2020).
- [53] A. Peruzzo, J. McClean, P. Shadbolt, M.-H. Yung, X.-Q. Zhou, P. J. Love, A. Aspuru-Guzik, and J. L. O’Brien, *Nature communications* **5**, 4213 (2014).
- [54] N. Suri, F. C. Binder, B. Muralidharan, and S. Vinjanampathy, *The European Physical Journal Special Topics* **227**, 203 (2018).

A. Description of Algorithmic Primitives

Here we describe in detail the algorithms for estimating overlaps (Algorithm 1) and transition amplitudes using LCU (Algorithm 2.1) and Block Encoding (Algorithm 2.2).

Algorithm 1 OEA

1. Given states $|x\rangle = (|0\rangle|\psi(t)\rangle + |1\rangle|\chi(t)\rangle)/\sqrt{2}$ and $|x'\rangle = |0\rangle|\psi(t)\rangle - i|1\rangle|\chi(t)\rangle/\sqrt{2}$.
2. Apply $H \otimes \mathbb{I}$ on $|x\rangle$ and $|x'\rangle$.
3. Measure the ancilla qubits of $|x\rangle$ and $|x'\rangle$ in the standard basis and estimate the probability of obtaining $|1\rangle$ by performing m repetitions. Let these probabilities be P_x and $P_{x'}$ respectively.
4. The overlap $\langle\psi(t)|\chi(t)\rangle$ can be computed as

$$\text{Re}(\langle\psi(t)|\chi(t)\rangle) = 2P_x - 1,$$

$$\text{Im}(\langle\psi(t)|\chi(t)\rangle) = 2P_{x'} - 1.$$

Algorithm 2.1 TAEA via LCU

1. Given a linear combination of unitaries $\mu = \sum_{j=1}^D c_j U_j$.
2. Estimate the overlap for each U_j

$$t_r^{(j)}, t_i^{(j)} \leftarrow \text{OVERLAP}(|\chi(t)\rangle, U_j |\psi(t)\rangle).$$

3. Combine these values to obtain

$$\text{Re}(\langle\chi(t)|\mu|\psi(t)\rangle) \leftarrow \sum_{j=1}^k c_j t_r^{(j)},$$

$$\text{Im}(\langle\chi(t)|\mu|\psi(t)\rangle) \leftarrow \sum_{j=1}^k c_j t_i^{(j)}.$$

Algorithm 2.2 TAEA via Block Encoding

1. Given an (α, k, ϵ) -block encoding B of μ defined according to [38].
2. Create the superposition

$$(|0\rangle|0_k\rangle|\psi(t)\rangle + |1\rangle|0_k\rangle|\chi(t)\rangle)/\sqrt{2},$$

and apply a conditional unitary B .

3. The transition amplitude can be computed as $\langle\chi(t)|\mu|\psi(t)\rangle = \alpha(\text{OVERLAP}(|0_k\rangle|\chi(t)\rangle, B|0_k\rangle|\psi(t)\rangle)$.
-

B. Quantum-Assisted GRAPE Algorithm

As another application of our algorithmic primitives, we discuss the implementation of the quantum-assisted GRAPE algorithm. GRAPE discretizes the time varying pulse into constant pulses over small time intervals of size Δt . Each piece-wise constant step is updated iteratively in a manner that monotonically increases the fidelity between the target state and evolved state. The unitary corresponding to the pulse sequence in the interval $j\Delta t \leq t < (j+1)\Delta t$ is $U_j = \exp\{-i\Delta t(H_0 + \sum_{k=1}^L u_k(j\Delta t)H_k)\}$. If we start with a state ρ_0 , the final evolved state is $\rho(T) = U_L \dots U_0 \rho_0 U_0^\dagger \dots U_L^\dagger$. Over each iteration, the update to $u_k(j\Delta t)$ is given by $\Delta u_k(j\Delta t) \propto \partial\phi_0/\partial u_k(j\Delta t)$, where ϕ_0 is the quantity to minimize (infidelity say). The derivative can be written as [3]

$$\frac{\partial\phi_0}{\partial u_k(j)} = -\text{tr}(\chi_j^\dagger i\Delta t[H_k, \rho_j])$$

where

$$\begin{aligned}\rho_j &= U_j \dots U_0 \rho_0 U_0^\dagger \dots U_j^\dagger \\ \chi_j &= U_{j+1}^\dagger \dots U_n^\dagger \rho_{tar} U_n \dots U_{j+1}\end{aligned}$$

and ρ_{tar} is the target state. GRAPE suffers from the same limitation as the Krotov method, which is that exponentially large resources are required to compute the evolution for large system sizes. However, this can be done in polynomial time even for many body systems by using DQS and extracting the gradients. The derivative can be computed as the difference between two SWAP tests [40]

$$\text{tr}(\chi_j^\dagger e^{i\Delta t} [(H_0 + H_k), \rho_j]) - \text{tr}(\chi_j^\dagger e^{i\Delta t} [H_0, \rho_j]) \approx -\text{tr}(\chi_j^\dagger e^{-i\Delta t(H_0+H_k)} \rho_j e^{i\Delta t(H_0+H_k)}) + \text{tr}(\chi_j^\dagger e^{-i\Delta t(H_0)} \rho_j e^{i\Delta t(H_0)}), \quad (9)$$

where terms of order higher than Δt have been ignored for the approximation.

C. Uniform Convergence Threshold for Noisy Quantum-Assisted Krotov Algorithm

We now show that the quantum-assisted Krotov algorithm is monotonically convergent until the updates are of the same magnitude as the errors. Recall the cost function

$$J^{(k)} = |\langle \tau | U^{(k)} | \psi(0) \rangle|^2 - \alpha \Delta t \sum_{j=1}^n (\xi_j^{(k)})^2 \quad (10)$$

where k is the iteration number and $\xi_j^{(k)}$ is the value of the pulse between $(j-1)\Delta t$ and $j\Delta t$. The time evolution is implemented via DQS as a result of which an approximate unitary W is implemented in place of the actual unitary. We can write the incremental change of the cost function in our algorithm as

$$\Delta J^{(k)} = |\langle \tau | W^{(k)} | \psi(0) \rangle|^2 - |\langle \tau | W^{(k-1)} | \psi(0) \rangle|^2 - \alpha \Delta t \sum_{j=1}^n [(\xi_j^{(k)})^2 - (\xi_j^{(k-1)})^2] \quad (11)$$

The pulse update is estimated by running the TAEA and OEA and then computing:

$$\Delta \xi_j^{(k)} = \frac{-1}{\alpha} \text{Im}(\langle \psi^{(k-1)}(T) | \tau \rangle \langle \tau | W_{j,n}^{(k-1)} \mu W_{1,j}^{(k)} | \psi(0) \rangle) \quad (12)$$

where $W_{n_1, n_2}^{(k)}$ is the Trotterized implementation of $U_{n_1, n_2}^{(k)} = \prod_{m=n_1}^{n_2} \exp(-i\Delta t H^{(k)}(m\Delta t))$. Let $\langle \psi^{(k-1)}(T) | \tau \rangle = a_1 + ib_1$, where a_1 and b_1 are estimated using single qubits measurements in OE and hence are Gaussian random variables with a variance of σ_b^2/m , where σ_b^2 is the variance of the Bernoulli random variable corresponding to the outcome of a projective measurement on the qubit and m is the number of measurements or samples. Similarly, if $\langle \tau | W_{j,n}^{(k-1)} \mu W_{1,j}^{(k)} | \psi(0) \rangle = a_2 + ib_2$, then the variance of a_2, b_2 depends on the technique used for TAE. If the LCU technique is used it is $(\sum_{l=1}^D c_l^2) \sigma_b^2/m = c^2 \sigma_b^2/m$. Here we have ignored second order terms that originate from errors introduced in the current iteration. Then

$$\Delta \xi_j^{(k)} = -\frac{1}{\alpha} (a_1 b_2 + a_2 b_1)$$

By using the properties of variances ($\text{Var}(XY) = \text{Var}(X)\text{Var}(Y) + \text{Var}(X)\text{Eva}(Y)^2 + \text{Var}(Y)\text{Eva}(X)^2$) it can be seen that the variance of $\Delta \xi_j^{(k)}$ is

$$\begin{aligned}\text{Var}(\Delta \xi_j^{(k)}) &= \frac{\sigma_b^2}{\alpha^2 m} (c^2 \langle a_1 \rangle^2 + \langle a_2 \rangle^2 + c^2 \langle b_1 \rangle^2 + \langle b_2 \rangle^2 + \frac{2c^2 \sigma_b^2}{m}) \\ &\leq \frac{1}{4\alpha^2 m} (c^2 + \|\mu\|^2)\end{aligned} \quad (13)$$

where we used $|\langle \tau | W_{j,n}^{(k-1)} \mu W_{1,j}^{(k)} | \psi(0) \rangle|^2 \leq \|\mu\|^2$, $|\langle \psi^{(k-1)}(T) | \tau \rangle|^2 \leq 1$, $\sigma_b^2 \leq 1/4$ and ignored $c^2/2m$ for the inequality.

We are yet to account for the error in the updates due to Trotterization. Since $\|U_{n_1, n_2}^{(k)} - W_{n_1, n_2}^{(k)}\| = \|\Delta U_{n_1, n_2}^{(k)}\| \leq \varepsilon_{TS}$,

$$\langle \tau | U_{j,n}^{(k-1)} \mu U_{1,j}^{(k)} | \psi(0) \rangle = \langle \tau | W_{j,n}^{(k-1)} \mu W_{1,j}^{(k)} | \psi(0) \rangle + \langle \tau | \Delta U_{j,n}^{(k-1)} \mu W_{1,j}^{(k)} | \psi(0) \rangle + \quad (14)$$

$$\langle \tau | W_{j,n}^{(k-1)} \mu \Delta U_{1,j}^{(k)} | \psi(0) \rangle + \langle \tau | \Delta U_{j,n}^{(k-1)} \mu \Delta U_{1,j}^{(k)} | \psi(0) \rangle. \quad (15)$$

We know that $|\langle a | \mu \Delta U | b \rangle| \leq \varepsilon_{TS} \|\mu\|$, then

$$|\text{Im}(\langle \psi(0) | U^{(k-1)\dagger} | \tau \rangle \langle \tau | U_{j,n}^{(k-1)} \mu U_{1,j}^{(k)} | \psi(0) \rangle) - \text{Im}(\langle \psi(0) | W^{(k-1)\dagger} | \tau \rangle \langle \tau | W_{j,n}^{(k-1)} \mu W_{1,j}^{(k)} | \psi(0) \rangle)| \quad (16)$$

$$\leq |\langle \psi(0) | U^{(k-1)\dagger} | \tau \rangle \langle \tau | U_{j,n}^{(k-1)} \mu U_{1,j}^{(k)} | \psi(0) \rangle - \langle \psi(0) | W^{(k-1)\dagger} | \tau \rangle \langle \tau | W_{j,n}^{(k-1)} \mu W_{1,j}^{(k)} | \psi(0) \rangle| \quad (17)$$

$$\leq 3\varepsilon_{TS} \|\mu\| \quad (\text{Ignoring higher order terms}) \quad (18)$$

Thus, an error δ_j^k such that $|\delta_j^k| \leq 3\varepsilon_{TS} \|\mu\| / \alpha$ is introduced in the updates due to Trotterization.

We can write $\Delta \xi_j^{(k)} = \langle \Delta \xi_j^{(k)} \rangle + \epsilon_j^k + \delta_j^k$ where ϵ_j^k is a random variable with the same distribution as $\Delta \xi_j^{(k)}$ but mean shifted to 0 and $\langle \circ \rangle$ denotes the stochastic average over noise realisations (Trotterization and measurement errors). Then from Chebyshev's inequality

$$\Pr[|\epsilon_j^k| \geq \varepsilon_M] \leq \frac{\text{Var}(\epsilon_j^k)}{N \varepsilon_M^2} \leq \frac{1}{4\alpha^2 m N \varepsilon_M^2} (c^2 + \|\mu\|^2) \quad (19)$$

where N is the number of samples of ϵ_j^k used for averaging. We have thus bounded both sources of errors.

These small fluctuations result in a slightly different unitary (before Trotterization) being chosen that can be described as follows

$$U^{(k)} = \prod_{j=1}^n e^{i\Delta t [H_0 + (\langle \xi_j^{(k)} \rangle + \epsilon_j^k + \delta_j^k) \mu]} \quad (20)$$

$$\approx \prod_{j=1}^n e^{i\Delta t [H_0 + (\langle \xi_j^{(k)} \rangle) \mu]} (\mathbb{I} + i\mu \Delta t (\epsilon_j^k + \delta_j^k)) \quad (21)$$

$$= \langle U^{(k)} \rangle + \sum_{j=1}^n i(\epsilon_j^k + \delta_j^k) \Delta t \mu^{j,k} \quad (22)$$

where we have ignored all terms of order larger than $\Delta t(\epsilon_j^k + \delta_j^k)$ and

$$\mu^{j,k} = \left(\prod_{j'=1}^{j-1} e^{i\Delta t [H_0 + (\langle \xi_{j'}^{(k)} \rangle) \mu]} \right) \mu \left(\prod_{j'=j+1}^n e^{i\Delta t [H_0 + (\langle \xi_{j'}^{(k)} \rangle) \mu]} \right)$$

The incremental change in cost function can then be written as

$$\begin{aligned}
\Delta J^{(k)} &= |\langle \tau | W^{(k)} | \psi(0) \rangle|^2 - |\langle \tau | W^{(k-1)} | \psi(0) \rangle|^2 - \alpha \Delta t \sum_{j=1}^n [(\xi_j^{(k)})^2 - (\xi_j^{(k-1)})^2] \\
&= |\langle \tau | \langle U^{(k)} \rangle | \psi(0) \rangle + \langle \tau | W^{(k)} - U^{(k)} | \psi(0) \rangle + \sum_{j=1}^n i(\epsilon_j^k + \delta_j^k) \Delta t \langle \psi(0) | \mu^{j,k} | \tau \rangle|^2 \\
&\quad - |\langle \tau | \langle U^{(k-1)} \rangle | \psi(0) \rangle + \langle \tau | W^{(k-1)} - U^{(k-1)} | \psi(0) \rangle + \sum_{j=1}^n i(\epsilon_j^{k-1} + \delta_j^{k-1}) \Delta t \langle \psi(0) | \mu^{j,k-1} | \tau \rangle|^2 \\
&\quad - \frac{\Delta t}{\alpha} \sum_{j=1}^n [(\langle \xi_k^{(j)} \rangle + \epsilon_j^k + \delta_j^k)^2 - (\langle \xi_{k-1}^{(j)} \rangle + \epsilon_j^{k-1} + \delta_j^{k-1})^2] \\
&\geq |\langle \tau | \langle U^{(k)} \rangle | \psi(0) \rangle|^2 + |\langle \tau | W^{(k)} - U^{(k)} | \psi(0) \rangle|^2 - |\langle \tau | \langle U^{(k-1)} \rangle | \psi(0) \rangle|^2 - |\langle \tau | W^{(k-1)} - U^{(k-1)} | \psi(0) \rangle|^2 \\
&\quad + |\sum_{j=1}^n (\epsilon_j^k + \delta_j^k) \Delta t \langle \psi(0) | \mu^{j,k} | \tau \rangle|^2 - |\sum_{j=1}^n (\epsilon_j^{k-1} + \delta_j^{k-1}) \Delta t \langle \psi(0) | \mu^{j,k-1} | \tau \rangle|^2 \\
&\quad - 2|\langle \tau | \langle U^{(k)} \rangle | \psi(0) \rangle| |\langle \tau | W^{(k)} - U^{(k)} | \psi(0) \rangle| - 2|\langle \tau | \langle U^{(k-1)} \rangle | \psi(0) \rangle| |\langle \tau | W^{(k-1)} - U^{(k-1)} | \psi(0) \rangle| \\
&\quad - 2|\langle \tau | \langle U^{(k)} \rangle | \psi(0) \rangle| |\sum_{j=1}^n (\epsilon_j^k + \delta_j^k) \Delta t \langle \psi(0) | \mu^{j,k} | \tau \rangle| \\
&\quad - 2|\langle \tau | \langle U^{(k-1)} \rangle | \psi(0) \rangle| |\sum_{j=1}^n (\epsilon_j^{k-1} + \delta_j^{k-1}) \Delta t \langle \psi(0) | \mu^{j,k-1} | \tau \rangle| \\
&\quad - 2|\langle \tau | W^{(k)} - U^{(k)} | \psi(0) \rangle| |\sum_{j=1}^n (\epsilon_j^k + \delta_j^k) \Delta t \langle \psi(0) | \mu^{j,k} | \tau \rangle| \\
&\quad - 2|\langle \tau | W^{(k-1)} - U^{(k-1)} | \psi(0) \rangle| |\sum_{j=1}^n (\epsilon_j^{k-1} + \delta_j^{k-1}) \Delta t \langle \psi(0) | \mu^{j,k-1} | \tau \rangle| \\
&\quad - \frac{\Delta t}{\alpha} \sum_{j=1}^n [(\langle \xi_k^{(j)} \rangle)^2 - (\langle \xi_{k-1}^{(j)} \rangle)^2 + (\epsilon_j^k + \delta_j^k)^2 - (\epsilon_j^{k-1} + \delta_j^{k-1})^2 + 2\langle \xi_k^{(j)} \rangle (\epsilon_j^k + \delta_j^k) - 2\langle \xi_{k-1}^{(j)} \rangle (\epsilon_j^{k-1} + \delta_j^{k-1})]
\end{aligned} \tag{23}$$

$$\tag{24}$$

$$\tag{25}$$

where we used $|a|^2 + |b|^2 + |c|^2 - 2|a||b| - 2|b||c| - 2|c||a| \leq |a + b + c|^2 \leq (|a| + |b| + |c|)^2$ for the inequality. In [2], it was shown that the (error-free) Krotov algorithm is monotonically convergent [54], namely

$$\langle \Delta J^{(k)} \rangle = |\langle \tau | \langle U^{(k)} \rangle | \psi(0) \rangle|^2 - |\langle \tau | \langle U^{(k-1)} \rangle | \psi(0) \rangle|^2 - \frac{\Delta t}{\alpha} \sum_{j=1}^n [(\langle \xi_k^{(j)} \rangle)^2 - (\langle \xi_{k-1}^{(j)} \rangle)^2] > 0. \tag{26}$$

However, if the fluctuations in $\Delta J^{(k)}$ due to measurement and Trotter errors, overwhelm $\langle \Delta J^{(k)} \rangle$, it is no longer possible to reliably achieve better results. Concretely, if

$$\langle \Delta J^{(k)} \rangle \gg 4T(\varepsilon_M + 3\varepsilon_{TS} \|\mu\|/\alpha) \|\mu\| + 4\frac{T}{\alpha} [\xi_{max}(\varepsilon_M + 3\varepsilon_{TS} \|\mu\|/\alpha)] + 4\varepsilon_{TS} \tag{27}$$

where $\xi_{max} = \max_j(\xi_j^{(k)}, \xi_j^{(k-1)})$ is the maximum amplitude of the pulse (can be upperbounded by experimental constraints), then with very high probability the fluctuations are much smaller than the actual update and monotonicity is guaranteed. Eq. (27) follows from the fact that the variance is upperbounded by ε_M with high probability and $\|W - U\| \leq \varepsilon_{TS}$. We have also dropped terms of higher order from the expression. Writing $\varepsilon = \varepsilon_M + 3\varepsilon_{TS} \|\mu\|/\alpha$, we get Eq.(8) in the main text.

In practice, one would first choose how ‘‘close’’ they wish to get to a target state by fixing a value ΔJ_{min} beyond which they stop the quantum control optimization. Once this is fixed, ε_M and ε_{TS} are chosen subject to experimental constraints using which the number of measurements/gates needed can be calculated using Eq. (19) and the results on Trotterization from [41] (see section on robustness in main text).